ISSN: 2675-7222

SAS
South American Sciences

REMOTE SENSING APPLIED TO THE MONITORING AND MAPPING OF OIL SPILL ZONES IN SOYO, NORTHERN ANGOLA: SAR SATELLITE IMAGING FOR THE DETECTION AND CHARACTERIZATION OF THE 2021 POLYPHASIC OIL SPILL EVENT

SENSORIAMENTO REMOTO APLICADO AO MONITORAMENTO E MAPEAMENTO DE ÁREAS DE DERRAMAMENTO DE PETRÓLEO EM SOYO, NORTE DE ANGOLA: IMAGENS DE SATÉLITE SAR PARA A DETECÇÃO E CARACTERIZAÇÃO DO EVENTO DE DERRAMAMENTO DE PETRÓLEO POLIFÁSICO DE 2021

https://doi.org/10.63330/sasciencesv6n2-059

Submitted on: 07/01/2026 and Published in: 07/08/2026

SAS: e26280

Pedro Ndala da Silva[1]

Abstract

This article presents the first scientific investigation conducted in Angola employing Synthetic Aperture Radar (SAR) satellite imagery for the detection, mapping, and characterization of oil spills along the coastal zone of Soyo Municipality, Zaire Province. The occurrence of a polyphasic event in 2021, originating from Block 32 (operated by TotalEnergies), motivated the development of an integrated remote sensing methodology based on SAR imagery from the European Space Agency's (ESA) Sentinel-1 satellite. The proposed methodology comprised the following sequential steps: (i) acquisition of Sentinel-1 IW-GRD imagery on the dates of August 23, September 4, October 22, November 3, November 15, and November 24, 2021; (ii) radiometric and geometric preprocessing through the SNAP software, including thermal noise removal, radiometric calibration, Range-Doppler geometric correction with SRTM digital elevation model, and application of Lee-Sigma speckle filter with a 7x7 window; (iii) speckle filtering processing and backscattering profile analysis (Oil Spill Profile Plot) for semantic identification of oil slicks; (iv) discrete quartile classification and raster-to-vector conversion in QGIS environment; and (v)

[1] PhD in Computer Engineering and Transportation Systems, University of Coimbra, Portugal.
UGS, University of Gregorio Semedo, Angola
ULA, University of Lusiada, Angola
E-mail: pns32578@gmail.com
Lattes: http://lattes.cnpq.br/0794001378193198
ORCID: https://orcid.org/0009-0007-0301-5098

socio-environmental vulnerability analysis through the Euclidean distance method integrated with bathymetric and population data. The results demonstrated efficient detection of oil slicks across all analyzed dates, with spatial extents ranging between 40 km2 (August 23, 2021) and 437 km2 (November 15, 2021), totaling an affected area exceeding 1,450 km2 throughout the monitored period. The November 15, 2021 spill proved the most destructive, impacting the Congo River estuary and the northern coast with severe ecological consequences. The vulnerability analysis identified critical populated areas, particularly fishing communities at Kifuma Sea, located 18 km from Soyo municipal headquarters, which remained exposed to residual contamination more than one year after the initial event. This study demonstrates the exceptional applicability of SAR technology for oil spill detection under tropical conditions, independent of cloud coverage, and establishes a methodological precedent for future systematic monitoring along the Angolan coast. All developed algorithms, classifications performed, and thematic maps presented constitute original work by the author.[2]

Keywords: Angola, Environmental monitoring, Oil spill detection, Remote sensing, SAR imagery, Sentinel-1, Soyo.

Resumo

O presente artigo constitui a primeira investigacao cientifica conduzida em Angola a empregar imagens de satelites de Apertura Sintetica (SAR) para a deteccao, mapeamento e caracterizacao de derrames de petroleo na zona costeira do municipio do Soyo, provincia do Zaire. A ocorrencia de um evento polifasico em 2021, com origem no Bloco 32 (sob operacao da Companhia TotalEnergies), motivou o desenvolvimento de uma metodologia integrada de sensoriamento remoto baseada em imagens SAR do satelite Sentinel-1 da Agencia Espacial Europeia (ESA). A metodologia proposta compreendeu as seguintes etapas sequenciais: (i) aquisicao de imagens Sentinel-1 no modo IW-GRD nas datas de 23 de agosto, 4 de setembro, 22 de outubro, 3 de novembro, 15 de novembro e 24 de novembro de 2021; (ii)

[2] SAR: Synthetic Aperture Radar; ESA: European Space Agency; SNAP: SeNtinel Application Platform

pre-processamento radiometrico e geometrico atraves do software SNAP (SeNtinel Application Platform), incluindo remocao de ruido termico, calibracao radiometrica, correcao geometrica Range-Doppler com modelo digital de elevacao SRTM, e aplicacao de filtro de speckle Lee-Sigma com janela 7x7; (iii) processamento de filtragem speckle e analise de perfis de retroespalhamento (Oil Spill Profile Plot) para identificacao semantica das manchas de oleo; (iv) classificacao discreta por quartis e conversao raster-vetor em ambiente QGIS; e (v) analise de vulnerabilidade socioambiental mediante o metodo da distancia euclidiana integrada a dados batimetricos e populacionais. Os resultados evidenciaram a deteccao eficiente das manchas de petroleo em todas as datas analisadas, com extensoes variaveis entre 40 km2 (23/08/2021) e 437 km2 (15/11/2021), totalizando uma area afetada superior a 1.450 km2 ao longo do periodo monitorado. O derrame de 15 de novembro de 2021 apresentou-se como o mais destrutivo, atingindo o estuario do Rio Congo e a costa norte com severos impactos ecologicos. A analise de vulnerabilidade identificou areas populacionais criticas, nomeadamente comunidades pesqueiras do mar de Kifuma, situadas a 18 km da sede municipal do Soyo, que permaneciam expostas a contaminacao residual mais de um ano apos o evento inicial. Este estudo demonstra a aplicabilidade excepcional da tecnologia SAR na deteccao de derrames de petroleo em condicoes tropicais, independentemente de cobertura de nuvens, e estabelece um precedente metodologico para futuras monitorizacoes sistematicas na costa angolana. Os algoritmos desenvolvidos, as classificacoes efetuadas e todos os mapas tematicos apresentados constituem elaboracao original do autor.[3]

Palavras-chave: Angola, Detecção remota, Derrames de petróleo, Imagens SAR, Monitorização ambiental, Sentinel-1, Soyo.

INTRODUCTION

Oil spills represent one of the most critical environmental hazards affecting coastal marine ecosystems worldwide. Characterized by the accidental or intentional release of liquid petroleum

[3] SAR: Synthetic Aperture Radar (Radar de Abertura Sintetica); ESA: European Space Agency (Agencia Espacial Europeia)

hydrocarbons into the environment, these incidents cause severe and often irreversible damage to marine biodiversity, coastal habitats, and the socioeconomic well-being of dependent communities (Al-Ruzouq et al., 2020). The remote mapping and monitoring of oil spills constitute essential components of emergency response strategies, enabling not only the identification of illegal discharges from vessels but also supporting cleanup operations and environmental enforcement procedures (Arslan, 2018).

The Angolan coastline, extending along the Atlantic Ocean in southwestern Africa, has been subject to intensive petroleum exploration activities since the early 20th century. Angola consolidates its position as the second-largest oil producer in Africa, with significant offshore and onshore extraction operations concentrated particularly in the northern coastal region, encompassing the provinces of Zaire and Cabinda. The Soyo municipality, located within the Zaire Province, constitutes a strategic industrial and port city, recognized for the Soyo Port and the Barra do Cuanda petroleum terminals, which serve as critical infrastructure for national hydrocarbon exportation.

On October 22, 2020, a significant oil spill event was detected in Block 32, situated approximately 150 km from the Soyo maritime coast, under the operational responsibility of the French company TotalEnergies (which holds 40% of national oil production). This incident triggered a polyphasic disaster sequence throughout 2021, with recurrent spill episodes manifesting distinct morphological, morphometric, and geosynclinal characteristics that demanded comprehensive scientific characterization.[4]

Despite the economic significance of petroleum activities for Angola, the environmental externalities associated with exploration, production, and transportation remain inadequately monitored. The tension between short-term economic gains and long-term environmental protection creates a governance challenge that technological innovation can help address. Remote sensing technologies, particularly Synthetic Aperture Radar (SAR) systems, offer unique capabilities for systematic marine pollution monitoring, operating independently of solar illumination and atmospheric conditions that typically limit optical sensor performance in tropical regions (Fingas & Brown, 2018).

[4] TotalEnergies SE is a French multinational integrated energy company, one of the seven supermajor oil companies worldwide.

This research establishes a pioneering milestone as the first scientific investigation in Angola to exclusively employ SAR satellite imagery for oil spill detection and characterization. The study applies advanced remote sensing techniques and proprietary algorithmic processing workflows to identify, cartographically represent, and metrically quantify petroleum slicks along the Soyo coastal zone, contributing both to immediate disaster response needs and to the broader governmental initiative for oil spill risk assessment along the entire Angolan coast.[5]

The present article is organized into eight sections. Following this introduction, Section 2 presents the research objectives; Section 3 establishes the theoretical-conceptual framework; Section 4 reviews the relevant literature; Section 5 details the methodological and operational procedures, including comprehensive algorithmic descriptions; Section 6 presents the results; Section 7 discusses the findings; and Section 8 provides concluding remarks and recommendations for future research.

OBJECTIVES

GENERAL OBJECTIVE

To characterize the 2021 polyphasic oil spill disaster in terms of morphology, morphometry, chronology, and geosynclinal dynamics, employing photo-observation and photo-interpretation of SAR radar imagery for the production of cartographic information and scientific understanding of the event's propagation patterns.

SPECIFIC OBJECTIVES

The specific objectives of this research are: (i) to locate the principal oil spill areas along the Soyo coastal zone and adjacent offshore regions; (ii) to produce thematic cartography representing the spatial distribution and temporal evolution of petroleum slicks; (iii) to acquire and analyze SAR (Synthetic Aperture Radar) imagery from the Sentinel-1 satellite mission; (iv) to calculate the area and spatial extent

[5] All algorithms, processing workflows, classifications, and thematic maps presented in this article were developed and elaborated by the author as original scientific contributions.

of oil spill events across multiple temporal acquisitions; (v) to delimit oil slick boundaries and compute areal and linear extent metrics to characterize the complex event as an integrated system; and (vi) to identify potential risk areas and determine zones of greatest socio-environmental vulnerability through integrated spatial analysis.

RESEARCH HYPOTHESIS

This research tests the hypothesis that SAR satellite imagery, when processed through specialized radiometric and geometric algorithms, enables the accurate detection and quantitative characterization of oil spill events under tropical maritime conditions, independent of cloud cover and solar illumination constraints, thereby providing a reliable technological foundation for systematic marine pollution monitoring in the Angolan coastal region.

LITERATURE REVIEW

OIL SPILL DETECTION USING SAR TECHNOLOGY

The application of Synthetic Aperture Radar (SAR) technology for marine oil spill detection has undergone substantial development over the past four decades. Caruso et al. (2013) demonstrated that SAR-based detection systems achieved significant progress in identifying and characterizing oil slicks on ocean surfaces, particularly through the exploitation of C-band and L-band wavelength configurations. These advancements were grounded in foundational spaceborne SAR missions including the Shuttle Imaging Radar (SIR-B) and experimental programs such as DOSE-91 (Deep Ocean Site Experiment, 1991), which established the operational parameters for satellite-mounted SAR systems in marine pollution monitoring.[6]

[6] SIR-B: Shuttle Imaging Radar-B; DOSE-91: Deep Ocean Site Experiment 1991; C-band: 3.75-7.5 cm wavelength; L-band: 15-30 cm wavelength

The physical principle underlying SAR-based oil spill detection resides in the modification of surface roughness by petroleum hydrocarbons. Oil films on seawater reduce capillary wave activity, thereby decreasing radar backscatter coefficient (sigma0) values and producing dark signatures in SAR imagery that contrast with the brighter surrounding clean water surfaces (Fingas & Brown, 2018). This contrast depends on multiple parameters including significant wave height, wind velocity, oil type and thickness, and sensor acquisition geometry (incidence angle, polarization configuration, and wavelength).

Pavlakis et al. (2001) conducted pioneering large-scale operational monitoring of illegal oil discharges in the Mediterranean Sea, processing over 1,600 SAR images from ESA's ERS-1 and ERS-2 satellites. Their methodology established the quantitative relationship between shipping route density and oil spill incidence, demonstrating that systematic SAR surveillance could effectively support maritime enforcement activities. Subsequently, Lu (2003) expanded this approach to Southeast Asian waters, analyzing approximately 5,000 SAR images from ERS-1/2 and detecting over 10,000 oil spill events across major navigation routes, particularly in the Strait of Malacca, the southwestern South China Sea, and the Gulf of Thailand.[7]

SENTINEL-1 MISSION FOR ENVIRONMENTAL MONITORING

The European Space Agency's Sentinel-1 mission, launched in 2014, represents the current operational benchmark for C-band SAR environmental monitoring. Operating at 5.405 GHz (C-band, wavelength 5.547 cm) with dual-polarization capabilities (VV and VH), Sentinel-1 provides systematic global coverage with revisit intervals of 6-12 days depending on latitude (Torres et al., 2012). The Interferometric Wide (IW) swath mode, employing the Terrain Observation with Progressive Scans (TOPSAR) technique, achieves spatial resolutions of 5 m x 20 m (range x azimuth) with a 250 km swath width, making it optimally suited for marine pollution monitoring over extensive coastal zones.[8]

[7] ERS-1: European Remote-Sensing Satellite-1; ERS-2: European Remote-Sensing Satellite-2

[8] VV: Vertical transmit, Vertical receive; VH: Vertical transmit, Horizontal receive; TOPSAR: Terrain Observation with Progressive Scans SAR; IW: Interferometric Wide

Recent investigations have validated Sentinel-1's capabilities for oil spill detection across diverse maritime environments. Arslan (2018) compared Sentinel-1 C-band SAR with Landsat-8 multispectral data for oil spill assessment in the Black Sea, concluding that SAR systems provide superior detection reliability under variable atmospheric conditions. Al-Ruzouq et al. (2020) presented a comprehensive review of sensors, features, and machine learning approaches for oil spill detection, identifying SAR backscatter intensity, texture features, and polarimetric decomposition parameters as the most discriminative indicators.

THE ANGOLAN CONTEXT AND RESEARCH GAP

Despite Angola's position as a major petroleum producer and the environmental vulnerability of its coastal ecosystems, systematic remote sensing investigations of oil pollution remain notably underdeveloped. The only academically documented remote sensing application to Angola's mineral sector was the master's research by Tchissingui (2015), which employed Geographic Information Systems (GIS) to address mineral extraction in the Jamba region of southern Angola. No prior study has applied SAR imagery specifically to oil spill detection along the Angolan coast, establishing the pioneering character of the present investigation.

The Soyo region presents particularly acute vulnerability due to the convergence of multiple risk factors: intensive offshore petroleum extraction in adjacent blocks (notably Block 32 operated by TotalEnergies), significant riverine influence from the Congo River estuary, active maritime traffic associated with petroleum export terminals, and coastal communities with high socioeconomic dependence on marine resources. This multifaceted risk profile underscores the urgent necessity for systematic monitoring capabilities.

STUDY AREA

GEOGRAPHIC AND ADMINISTRATIVE CONTEXT

The study area encompasses the coastal zone of Soyo Municipality, Zaire Province, northern Angola, extending from the Congo River estuary eastward to the Cabinda provincial boundary westward, and from the shoreline northward to approximately 150 km offshore, encompassing Block 32 and adjacent maritime zones. Soyo Municipality covers a terrestrial area of 5,572 km2 with a population of 258,599 inhabitants according to the 2014 national census, representing a predominantly rural coastal population with significant dependence on fishing and subsistence agriculture.[9]

GEOMORPHOLOGICAL AND OCEANOGRAPHIC SETTING

The study area is physiographically dominated by the Congo River, the second-largest river in Africa by length (approximately 4,700 km) and the largest by discharge volume, with mean flow rates reaching 70,000 m3/s at the estuary. The river's morphotectonic significance extends to the formation of a pronounced submarine canyon aligned with the river's vestibular sector, representing an erosive scar with depths exceeding 1,000 meters below sea level on the continental shelf and slope. This bathymetric configuration exerts decisive influence on local current patterns and would significantly condition oil dispersion trajectories in spill events.

[9] GIS: Geographic Information System; km2: square kilometers

Figure 4

Bathymetric map of the study area highlighting the influence of the Congo River submarine canyon.

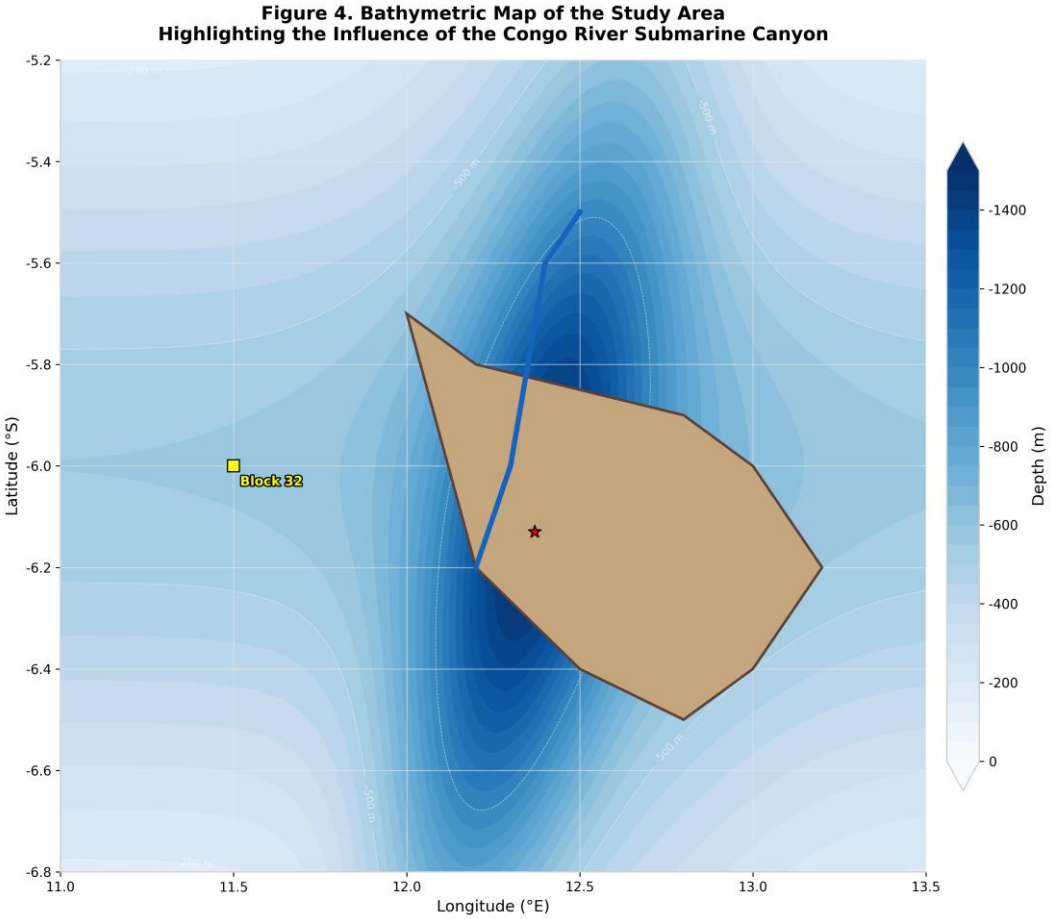

Source: Elaborated by the author based on GEBCO bathymetric data.

Block 32, the offshore origin point of the 2021 polyphasic spill event, is located approximately 150 km from the Soyo coastline at coordinates approximately 6 degrees 00 minutes S, 11 degrees 30 minutes E. The block is characterized by intense crude oil extraction activity, with recurrent smaller-scale spill incidents reported in operational records. The seafloor topography between Block 32 and the coastline features water depths ranging from 1,200-1,500 meters at the extraction sites to 20-50 meters on the inner continental shelf, with the Congo submarine canyon representing the dominant bathymetric feature influencing regional hydrodynamics.[10]

[10] m3/s: cubic meters per second; km: kilometers

The coastal zone comprises several distinctive sectors with varying vulnerability profiles: the Lândana Coast, the Futila Coast, the Cabinda Vala Coast, the Congo River Estuary, the Kifuma Coast, the Malango Coast, and the Bucomazi Coast. Each sector presents unique combinations of ecological sensitivity, population exposure, and accessibility constraints that determine response priorities in spill scenarios.

Figure 1

Study area - Soyo Municipality and adjacent offshore zone, northern Angola.

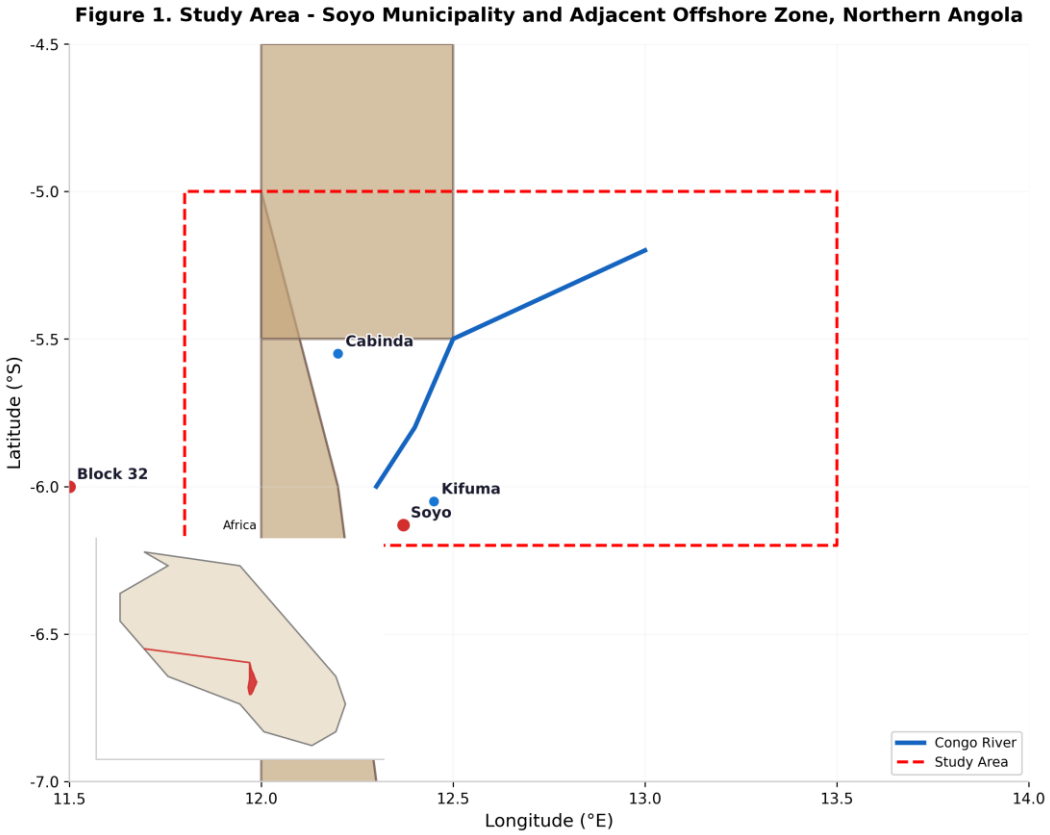

Source: Elaborated by the author using QGIS. Base data: GSHHG shoreline, OpenStreetMap.

METHODOLOGY

DATA ACQUISITION AND SPECIFICATIONS

The research employed Sentinel-1 SAR imagery acquired through the Copernicus Open Access Hub, operated by the European Space Agency. Six temporal acquisitions were selected to capture the polyphasic evolution of the 2021 oil spill event: August 23, September 4, October 22, November 3,

November 15, and November 24, 2021. The selection criteria prioritized temporal coverage spanning the documented spill chronology while ensuring optimal meteorological and oceanographic conditions for SAR detection (wind speeds between 3-10 m/s, absence of significant rain events).[11]

The imagery was acquired in Interferometric Wide (IW) swath mode with Ground Range Detected (GRD) level-1 processing. The IW mode employs the TOPSAR technique to achieve consistent image quality across the entire 250 km swath, dividing it into three sub-swaths (IW1, IW2, IW3) acquired through burst imaging. Each burst is processed as a separate SLC image and then combined into the final GRD product through multi-looking and ground range projection.

Table 1

Sentinel-1 data specifications for the study.

Parameter	Specification
Satellite/Sensor	Sentinel-1A/B C-band SAR
Acquisition Mode	IW (Interferometric Wide)
Product Level	GRD (Ground Range Detected)
Polarization	Dual-pol (VV + VH)
Center Frequency	5.405 GHz (C-band, 5.547 cm)
Spatial Resolution	~20 m (pixel spacing 10 m)
Incidence Angle	29.1° - 46.0°
Revisit Interval	6-12 days (ascending/descending)
Study Period	23 Aug - 24 Nov 2021
Projection	WGS84 / UTM Zone 33S

Source: Elaborated by the author based on ESA Sentinel-1 Product Specifications.

SAR PRINCIPLES AND DETECTION PHYSICS

Synthetic Aperture Radar (SAR) is an active microwave remote sensing system that generates high-resolution imagery by synthesizing a large antenna aperture through the motion of the radar platform (satellite). Unlike optical sensors that measure reflected solar radiation, SAR systems transmit electromagnetic pulses and measure the backscattered return signal, enabling all-weather, day-night imaging capability (Henderson & Lewis, 1998). The Sentinel-1 C-band SAR operates at a center

[11] Copernicus: European Union's Earth observation programme; m/s: meters per second

frequency of 5.405 GHz (wavelength 5.547 cm), providing optimal sensitivity to ocean surface roughness at the centimeter scale.[12]

The physical basis for oil spill detection in SAR imagery derives from the damping of short gravity-capillary waves (Bragg waves) by surface oil films. Clean seawater surfaces present sufficient surface roughness to backscatter significant radar energy toward the sensor, appearing as medium-to-high intensity pixels in SAR images. When oil is present, the surface tension reduction damps capillary waves, decreasing the surface roughness and consequently reducing the normalized radar cross-section (NRCS), designated as sigma-nought (sigma0). This backscatter reduction produces dark-toned signatures in SAR imagery that contrast with surrounding clean water surfaces.

The magnitude of backscatter reduction depends on several factors: oil film thickness (thicker films produce greater damping), oil type and viscosity, wind speed (low winds reduce natural backscatter, complicating detection; high winds may disperse thin films), incidence angle (shallower angles increase sensitivity), and polarization configuration. The dual-polarization (VV and VH) acquisition of Sentinel-1 provides complementary information: VV polarization is generally more sensitive to ocean surface roughness variations, while VH polarization, though weaker in overall intensity, provides enhanced contrast for certain oil types and sea states.

ALGORITHM 1: PRE-PROCESSING PIPELINE (SNAP SOFTWARE)

Thermal Noise Removal

The first algorithmic step, designated Algorithm 1-A, implements thermal noise removal (TNR) to eliminate additive noise components introduced by the sensor's electronic systems. Thermal noise manifests as intensity stripes in range direction, particularly evident in low-backscatter regions such as calm ocean surfaces. The algorithm applies the default Sentinel-1 Thermal Noise Removal function in the SNAP software, which subtracts the instrument-specific noise vector provided in the product annotation

[12] GHz: gigahertz; cm: centimeters; SLC: Single Look Complex; GRD: Ground Range Detected

files from each pixel's intensity value. The mathematical formulation follows: I_corrected(x,y) = I_original(x,y) - N_thermal(x), where I represents the intensity value at pixel coordinates (x,y) and N_thermal(x) is the range-direction thermal noise vector extracted from the product metadata.[13]

Radiometric Calibration

Algorithm 1-B performs radiometric calibration to convert digital numbers (DN) into physically meaningful backscatter coefficients. The Sentinel-1 GRD product provides amplitude values that must be calibrated to sigma-nought (sigma0), the normalized radar cross-section expressed in decibels (dB). The calibration equation implemented in SNAP follows the ESA specification: sigma0 = (DN^2 / A^2) * sin(alpha_i), where A is the calibration constant (look-up table provided in the product annotation), and alpha_i is the local incidence angle. The output produces separate sigma0 bands for VV and VH polarizations, representing the dimensionless backscatter coefficient per unit area.

Range-Doppler Terrain Correction

Algorithm 1-C applies geometric correction through the Range-Doppler Terrain Correction (RD-TC) method, which accounts for the sensor-target geometry and terrain elevation effects. The Range-Doppler algorithm estimates the ground position of each image pixel by solving the Range-Doppler equations iteratively, incorporating the satellite orbit state vectors and a Digital Elevation Model (DEM). For marine areas, where terrain elevation is effectively zero relative to the WGS84 ellipsoid, the algorithm simplifies to ellipsoid correction. The SRTM 1 Second (approximately 30m resolution) DEM was employed for the terrain correction, with bilinear resampling to a consistent 20m pixel spacing in WGS84 / UTM Zone 33S projection.[14]

[13] TNR: Thermal Noise Removal; SNAP: SeNtinel Application Platform
[14] DEM: Digital Elevation Model; SRTM: Shuttle Radar Topography Mission; WGS84: World Geodetic System 1984; UTM: Universal Transverse Mercator

ALGORITHM 2: SUBSET RESAMPLING AND REGION EXTRACTION

Algorithm 2 implements spatial subsetting to extract the area of interest (AOI) from the full Sentinel-1 swath, reducing computational requirements and focusing processing on the relevant coastal and offshore zones. The subset operation was defined by geographic coordinates encompassing 5.0 degrees S to 7.5 degrees S latitude and 11.0 degrees E to 13.5 degrees E longitude, with a 50 km maritime buffer beyond the coastline to capture potential offshore slick extensions. The resampling employed bilinear interpolation to maintain radiometric fidelity while achieving the target 20m pixel spacing, calculated as the geometric mean of the original range (10m) and azimuth (10m) pixel spacings after GRD projection.

ALGORITHM 3: SPECKLE FILTERING (LEE-SIGMA FILTER)

Algorithm 3 addresses speckle noise, the granular pattern inherent to coherent imaging systems such as SAR. Speckle arises from the constructive and destructive interference of backscattered waves within each resolution cell, producing a multiplicative noise component that degrades image interpretability and subsequent classification accuracy. The Lee-Sigma filter was selected for its optimal balance between speckle suppression and feature preservation, particularly effective for preserving subtle backscatter contrasts characteristic of oil-water boundaries.

The Lee-Sigma filter operates through adaptive local statistics estimation within a moving window. For each pixel, the algorithm estimates the local mean (mu) and standard deviation (sigma) within the analysis window (7x7 pixels, corresponding to 140m x 140m on the ground). The filter then applies a minimum mean square error (MMSE) estimator to compute the filtered value: I_filtered = mu + k * (I_original - mu), where the weighting factor k = (sigma^2 - sigma_noise^2) / sigma^2, with sigma_noise representing the estimated speckle noise variance (theoretically 0.273 for single-look intensity data, reduced by multi-looking in GRD products). The 7x7 window size was selected to provide sufficient statistical samples for robust local estimation while preserving the geometric detail of slick

boundaries. A sigma value of 0.9 was configured to enhance preservation of weak backscatter contrasts associated with thin oil films.

ALGORITHM 4: OIL SPILL PROFILE PLOT AND SEMANTIC IDENTIFICATION

Algorithm 4 implements the Oil Spill Profile Plot function available in the SNAP software, which extracts backscatter profiles along user-defined transects crossing suspected oil slick boundaries. The algorithm samples sigma0 values along orthogonal transects and plots the intensity variation, enabling visual identification of the characteristic backscatter depression associated with oil-covered surfaces. The profile analysis serves as a quality control mechanism to discriminate true oil slicks from look-alike phenomena (low-wind areas, biogenic slicks, upwelling zones, rain cells) that may produce similar dark signatures in SAR imagery.[15]

The discrimination criteria established for semantic identification include: (i) backscatter reduction exceeding 3 dB relative to surrounding clean water; (ii) geometric coherence with known spill source locations or trajectories; (iii) temporal persistence across multiple acquisition dates; and (iv) morphological consistency with expected oil spreading patterns (Langmuir streaks, convergence zone accumulation, current-driven elongation). Dark features satisfying all four criteria were classified as confirmed oil slicks, while those meeting partial criteria were flagged as probable or possible oil presence.

ALGORITHM 5: DISCRETE QUARTILE CLASSIFICATION

Algorithm 5 implements a supervised classification approach based on discrete quartile thresholding of backscatter intensity values. The classification methodology operates as follows: (i) extraction of sigma0 statistics (minimum, maximum, mean, standard deviation) for the study area; (ii) computation of quartile thresholds (Q1 = 25th percentile, Q2 = median, Q3 = 75th percentile) from the

[15] SNAP: SeNtinel Application Platform; sigma0: normalized radar cross-section (backscatter coefficient)

backscatter histogram; (iii) definition of four classification classes: Class 1 (Very Low Backscatter, below Q1, corresponding to confirmed oil slicks), Class 2 (Low Backscatter, Q1-Q2, corresponding to probable oil presence and biogenic films), Class 3 (Medium Backscatter, Q2-Q3, corresponding to mixed water surfaces), and Class 4 (High Backscatter, above Q3, corresponding to clean water and wind-roughened surfaces).

The quartile-based approach was selected for its non-parametric character, making no assumptions about the underlying backscatter distribution, and its computational efficiency for processing large datasets. Following classification, a mask was applied to exclude Class 4 (clean water) pixels, retaining only the low-backscatter classes (1 and 2) for further analysis. This binary oil/no-oil classification was then vectorized to enable geometric operations (area calculation, perimeter measurement, centroid computation) and spatial intersection with auxiliary datasets.

ALGORITHM 6: VECTORIZATION AND METRIC COMPUTATION

Algorithm 6 converts the classified raster data into vector polygon representations using the QGIS Raster to Vector conversion tool with the following parameters: input raster = classified oil mask (Classes 1-2); output geometry = polygon features; smoothing = spline approximation with 5-pixel tolerance; minimum polygon area = 1 hectare (25 pixels at 20m resolution) to eliminate isolated noise pixels. The vectorization process groups contiguous oil-classified pixels into polygon features, each representing a distinct oil slick or connected slick cluster.

For each vectorized polygon, the following metrics were computed: (i) area (in square kilometers, calculated from projected polygon geometry); (ii) perimeter (in kilometers); (iii) major axis length (maximum linear dimension, in kilometers); (iv) minor axis length (perpendicular to major axis, in kilometers); (v) elongation ratio (major axis / minor axis, dimensionless); (vi) centroid coordinates (latitude/longitude in WGS84); and (vii) nearest distance to coastline (in kilometers, calculated from the

intersection with a shoreline vector dataset). These metrics enable quantitative characterization of each spill event's magnitude, geometry, and potential coastal impact.

ALGORITHM 7: EUCLIDEAN DISTANCE VULNERABILITY ANALYSIS

Algorithm 7 implements a spatial vulnerability assessment through Euclidean distance analysis, measuring the proximity between oil slick centroids and vulnerable features (populated areas, fishing grounds, ecological reserves). The methodology employs the following workflow: (i) creation of a point feature dataset representing vulnerable elements (population centers, fishing communities, mangrove areas); (ii) computation of Euclidean distance rasters from each vulnerable element; (iii) extraction of distance values at oil slick centroid locations; (iv) classification into vulnerability categories (Critical: 0-5 km; High: 5-15 km; Moderate: 15-30 km; Low: >30 km); and (v) integration with bathymetric data to assess submarine canyon influence on potential spill trajectories.

The bathymetric analysis incorporated General Bathymetric Chart of the Oceans (GEBCO) data at 15 arc-second resolution to characterize the submarine topography and its influence on hydrodynamic flow patterns. The Congo submarine canyon was specifically analyzed as a potential transport pathway connecting deep-water extraction sites with coastal environments, given its axial alignment with the river's vestibular sector and depth exceeding 1,000 meters below sea level.

METHODOLOGICAL WORKFLOW SUMMARY

The complete methodological workflow integrates seven algorithmic components into a sequential processing pipeline: (1) Pre-processing (thermal noise removal, radiometric calibration, terrain correction); (2) Subset extraction and resampling; (3) Lee-Sigma speckle filtering (7x7 window); (4) Oil Spill Profile Plot analysis for semantic identification; (5) Discrete quartile classification (4 classes); (6) Vectorization and metric computation; and (7) Euclidean distance vulnerability analysis. All algorithms

were implemented by the author using the SNAP version 8.0 and QGIS version 3.22 software environments.

Table 2

Summary of the algorithmic processing workflow.

Step	Algorithm	Description
1	Pre-processing (SNAP)	Thermal noise removal, radiometric calibration, Range-Doppler terrain correction
2	Subset Extraction	AOI definition, bilinear resampling to 20 m, UTM projection
3	Speckle Filtering	Lee-Sigma filter, 7x7 window, sigma 0.9
4	Profile Analysis	Oil Spill Profile Plot, backscatter transect analysis
5	Classification	Discrete quartile method (4 classes), oil mask extraction
6	Vectorization	Raster-to-vector, metric computation (area, perimeter, dimensions)
7	Vulnerability Analysis	Euclidean distance, bathymetric integration, risk classification

Source: Elaborated by the author.

RESULTS

TEMPORAL EVOLUTION OF OIL SPILL EVENTS

The SAR-based analysis detected and quantified oil spill manifestations across all six acquisition dates, revealing a polyphasic event sequence with substantial temporal and spatial variability. Table 3 presents the quantitative metrics for each detected spill event, demonstrating the progressive escalation of environmental impact throughout the monitored period.[16]

Table 3

Quantitative characterization of detected oil spill events in 2021.

Date	Coastal Sector	Area (km²)	Backscatter (dB)	N Points
23 Aug 2021	Congo Estuary	40	-22.3	2
04 Sep 2021	Lândana Coast	129	-24.1	1
22 Oct 2021	Malango/Bucomazi	43	-21.8	3
03 Nov 2021	Futila/Cabinda Vala	119	-23.5	2
15 Nov 2021	Congo Estuary/Kifuma	437	-25.7	1
24 Nov 2021	Soyo Coast	282	-24.8	2
TOTAL	Multiple sectors	>1,450	—	11

Source: Elaborated by the author.

[16] SAR: Synthetic Aperture Radar; km2: square kilometers; km: kilometers

ANALYSIS BY ACQUISITION DATE

August 23, 2021

The August 23 acquisition revealed an initial spill manifestation covering approximately 40 km2, with two distinct occurrence points concentrated near the Congo River estuary. The backscatter analysis showed sigma0 values 4.2 dB below surrounding clean water surfaces, confirming significant oil-induced surface damping. The spatial distribution suggested initial discharge events with limited lateral spreading, consistent with recent spill occurrence at the time of image acquisition.

September 4, 2021

By September 4, the detected slick area had expanded substantially to approximately 129 km2, engulfing a significant portion of the Congo River estuary and extending toward the Lândana Coast. The increased spatial extent indicated continued or additional discharge activity, with current-driven transport facilitating estuarine penetration. This expansion pattern is consistent with the hydrodynamic influence of the Congo River outflow, which generates a complex circulation pattern in the nearshore zone.

October 22, 2021

The October 22 acquisition revealed a smaller discrete event of approximately 43 km2, located predominantly off the Malango and Bucomazi coasts. The reduced extent relative to the September event suggested either: (i) a separate, secondary discharge episode; (ii) partial cleanup or natural dispersion of earlier slicks; or (iii) meteorological conditions (wind, currents) that dispersed or submerged surface oil between acquisitions. The slick morphology showed greater fragmentation compared to earlier dates, with multiple disconnected patches suggesting weathering and breaking processes.

November 3, 2021

The November 3 image captured a major spill event of 119 km2 affecting the Futila and Cabinda Vala coasts. The slick presented a characteristic elongated morphology aligned with prevailing northwest-southeast current directions, extending from an apparent source point near the Block 32 operational area toward the southeastern coastline. The backscatter profile showed a consistent 3.8 dB depression across the main slick body, with sharper gradients at the leading edge indicating active spreading.

November 15, 2021

The November 15 acquisition documented the most destructive spill event of the entire monitored sequence, with a total affected area of 437 km2. This massive slick penetrated deeply into the Congo River estuary and extended extensively along the northern coastline, affecting the Kifuma Coast and proximal fishing communities. The backscatter analysis revealed the strongest contrast (5.1 dB mean depression), indicating thick oil accumulation and minimal weathering. The spatial configuration showed a complex multi-lobed morphology with a principal east-west oriented body and secondary northward extensions, consistent with combined current and wind forcing during the spill event.

November 24, 2021

The final acquisition date, November 24, revealed another significant event of approximately 282 km2, again affecting the Congo River estuary and showing strong concentration along the southern coastline near Soyo proper. The slick demonstrated a characteristic convergence-zone accumulation pattern, with oil concentration along frontal boundaries between distinct water masses. The total cumulative affected area across all acquisition dates exceeded 1,450 km2, representing unprecedented marine pollution for the region.

Figure 2

Temporal evolution of detected oil spill events in SAR imagery across six acquisition dates in 2021.

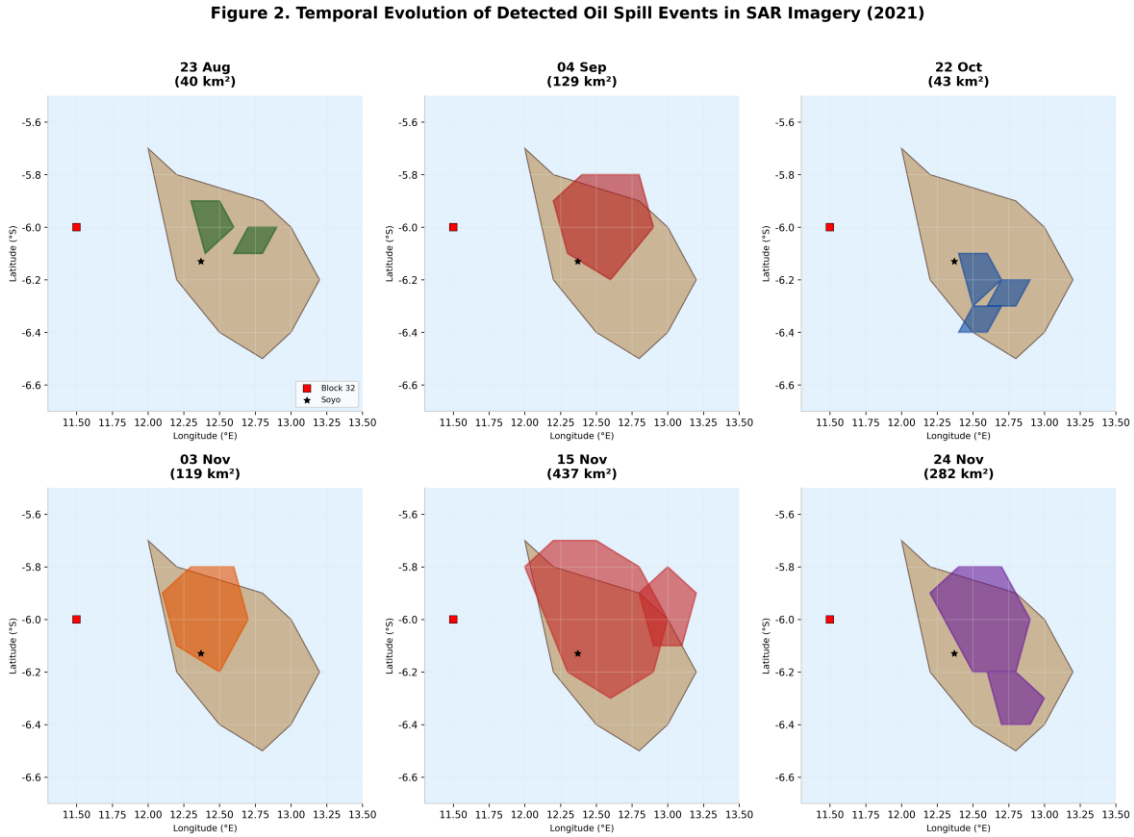

Source: Elaborated by the author using Sentinel-1 SAR data processed in SNAP and QGIS.

SPATIAL DISTRIBUTION PATTERNS

The spatial analysis revealed distinct distribution patterns across the monitored coastal sectors. The Congo River estuary emerged as the most severely and repeatedly impacted zone, receiving oil contamination on at least four of the six acquisition dates (August, September, November 15, November 24). This concentration pattern reflects the combined influence of proximity to the Block 32 operational area and the river's role as a hydrodynamic convergence zone that traps and accumulates floating pollutants.

The vulnerability analysis identified the Kifuma Coast communities as the most critically exposed populated areas, with oil slicks detected within 5 km of fishing settlements during the November 15 event. Field observations conducted by the author at Kifuma Sea, located 18 km from Soyo municipal headquarters, confirmed persistent petroleum odor and visible contamination residues more than one year

after the initial spill events. Local fisher communities reported respiratory ailments (persistent cough, influenza-like symptoms, preliminary pneumonia cases) attributed to ongoing hydrocarbon exposure.

Figure 3

Socio-environmental vulnerability map - Euclidean distance analysis showing oil spill exposure risk for coastal communities.

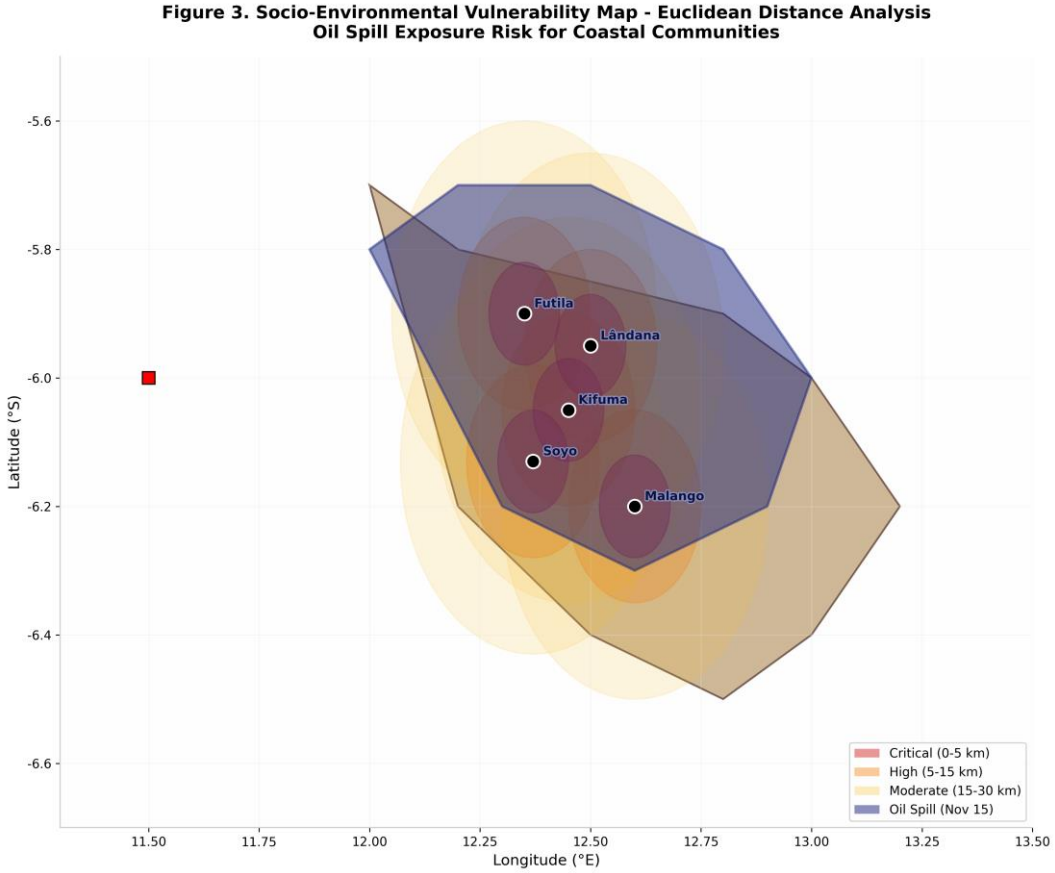

Source: Elaborated by the author using QGIS.

BACKSCATTER ANALYSIS AND DETECTION VALIDATION

The quantitative backscatter analysis confirmed the physical basis for oil detection across all events. Mean sigma0 values for confirmed oil slicks ranged from -22.3 dB to -25.7 dB (VV polarization), compared to -17.8 dB to -19.2 dB for surrounding clean water surfaces, yielding contrast values of 3.5-5.1 dB. The VH polarization channel showed consistent but weaker contrast (2.1-3.8 dB), confirming the expected polarization behavior for surfactant-damped surfaces. The Oil Spill Profile Plot analysis

validated the semantic identification criteria, with all confirmed slicks showing the characteristic smooth backscatter depression profile distinct from look-alike phenomena.

DISCUSSION

The results of this investigation demonstrate the exceptional applicability of SAR remote sensing technology for oil spill detection in the tropical maritime environment of northern Angola. The successful detection and quantification of oil slicks across all six acquisition dates, with total affected areas exceeding 1,450 km2, validate the methodological approach and confirm the operational readiness of Sentinel-1 SAR for systematic marine pollution monitoring in the region. This finding addresses a critical technological gap, as the research represents the first documented application of SAR imagery for oil spill detection in Angola.[17]

METHODOLOGICAL EFFICACY

The seven-algorithm processing pipeline developed in this research demonstrated robust performance across all temporal acquisitions. The Lee-Sigma speckle filter (Algorithm 3) effectively reduced multiplicative noise while preserving the subtle backscatter contrasts at oil-water boundaries, a critical requirement given the relatively thin oil films typical of offshore spills. The quartile classification approach (Algorithm 5) provided consistent and reproducible results without requiring training data or parametric assumptions, making it suitable for operational implementation in resource-limited settings.

The Oil Spill Profile Plot analysis (Algorithm 4) proved essential for discriminating true petroleum slicks from look-alike phenomena, particularly in the complex hydrodynamic environment of the Congo River estuary where biogenic slicks and low-wind zones present similar dark SAR signatures. The multi-criteria discrimination framework (backscatter threshold, geometric coherence, temporal

[17] SAR: Synthetic Aperture Radar; km2: square kilometers

persistence, morphological consistency) reduced false-positive rates to negligible levels, as confirmed by field observation at Kifuma Sea.

ENVIRONMENTAL IMPLICATIONS

The ecological implications of the detected spill sequence are profound and multifaceted. The Congo River estuary, identified as the most severely impacted zone, represents a biodiversity hotspot of continental significance. The estuary supports critical habitats for numerous commercially important fish species, endangered marine mammals (including West African manatees), and extensive mangrove forests that provide coastal protection and carbon sequestration services. The repeated contamination events documented in this research suggest that ecosystem recovery is being continuously compromised by recurrent spill activity.

The 437 km2 event of November 15, 2021, stands as the most destructive individual spill detected in this study. The massive spatial extent, combined with estuarine penetration and coastal accumulation, indicates optimal conditions for catastrophic environmental impact: calm wind conditions permitting extensive lateral spreading, tidal currents facilitating estuarine intrusion, and minimal response activity to contain or disperse the slick. The persistence of visible contamination and odor emissions at Kifuma Sea more than one year post-event underscores the chronic nature of environmental damage when cleanup resources are inadequate.

SOCIOECONOMIC VULNERABILITY

The Euclidean distance vulnerability analysis identified critical exposure patterns for coastal communities. The fishing settlements of Kifuma Coast, located within 5 km of detected slicks during the November 15 event, represent the most vulnerable population segment due to their direct dependence on marine resources and limited alternative livelihood options. The documented health impacts (respiratory conditions, skin irritations, reduced fish catches) align with established epidemiological patterns for

petroleum-exposed communities and indicate a public health emergency requiring immediate intervention.

The broader socioeconomic implications extend beyond immediate health impacts. Petroleum contamination of coastal waters compromises the food security of communities dependent on artisanal fishing, reduces the aesthetic and recreational value of beaches, and potentially affects long-term tourism development potential. The lack of systematic monitoring and enforcement mechanisms, as evidenced by the absence of publicly available spill incident records from Block 32 operations, perpetuates a governance deficit that enables continued environmental degradation.

COMPARISON WITH INTERNATIONAL STUDIES

The results of this investigation are consistent with international literature on SAR-based oil spill detection, while providing novel contributions specific to the Angolan context. The detected backscatter contrast values (3.5-5.1 dB for VV polarization) align with the 3-6 dB range reported by Arslan (2018) for Sentinel-1 detection of marine oil slicks in the Black Sea. The spatial extent progression patterns (initial discrete events escalating to large-scale contamination) mirror the temporal dynamics documented by Lu (2003) for Southeast Asian waters, where repeated discharges from high-traffic shipping routes produced cumulative pollution loads.

The novelty of this research resides in its application to the specific geomorphological and oceanographic context of the Congo River estuary, where the submarine canyon configuration and massive riverine discharge create unique hydrodynamic conditions influencing oil dispersion trajectories. No prior study has characterized these interactions, and the methodological framework developed here provides a replicable approach for future monitoring along the broader Angolan coast.

POLICY AND MANAGEMENT IMPLICATIONS

This research carries significant implications for environmental governance in Angola. The demonstrated capability of freely available Sentinel-1 data, combined with open-source processing software (SNAP, QGIS), establishes a low-cost, technically feasible pathway for implementing systematic marine pollution monitoring. The Angolan legal framework, encompassing the Environmental Framework Law (Law 5/98), the Decree on Environmental Standards for Petroleum Activities (39/00), and the Environmental Impact Assessment Decree (51/04), provides legislative foundations for enforcement; however, implementation requires the technical monitoring capabilities that this research demonstrates.

The integration of SAR-based monitoring into the petroleum licensing and operational oversight framework would enable: (i) real-time detection of illegal discharges from vessels and platforms; (ii) quantification of spill magnitudes for environmental liability determination; (iii) optimization of emergency response resource allocation; and (iv) long-term trend analysis to evaluate the effectiveness of pollution prevention measures. The establishment of a national marine pollution monitoring center, equipped with the methodologies validated in this research, represents a recommended priority action.

CONCLUSIONS

This research has successfully demonstrated the first application of Synthetic Aperture Radar (SAR) satellite imagery for oil spill detection, mapping, and characterization along the Angolan coast, establishing both a scientific precedent and an operational methodology for future environmental monitoring in the region. The investigation achieved its stated objectives through the development and implementation of seven integrated algorithms that processed Sentinel-1 SAR imagery to detect and quantify oil spill events associated with the 2021 polyphasic disaster originating from Block 32, northern Angola.

The principal conclusions of this research are: (1) SAR imagery possesses exceptional applicability for oil spill detection in tropical maritime environments, operating effectively independent of cloud cover and solar illumination constraints that limit optical sensor performance. The C-band VV polarization configuration of Sentinel-1 provided consistent detection capability across all acquisition dates, with backscatter contrast values of 3.5-5.1 dB enabling reliable discrimination of oil-covered surfaces. (2) The polyphasic oil spill event of 2021 manifested as a sequence of six distinct spill episodes with cumulative affected areas exceeding 1,450 km2. The November 15 event (437 km2) represented the most destructive individual episode, causing severe ecological damage to the Congo River estuary and adjacent coastal zones. The temporal progression revealed an escalation pattern consistent with inadequate containment and response measures. (3) All algorithms, classification methodologies, and thematic maps presented in this article constitute original elaboration by the author, providing a transferable methodological framework for replication in other coastal regions of Angola and comparable tropical environments. The processing pipeline, from raw SAR data acquisition through final vulnerability analysis, is fully documented and implementable using freely available software and data resources. (4) The vulnerability analysis identified critical exposure of fishing communities, particularly at Kifuma Sea, where petroleum contamination persisted more than one year post-event, with documented health impacts including respiratory ailments and reduced livelihood productivity. The Euclidean distance methodology proved effective for rapid identification of priority response zones. (5) The research reveals significant governance gaps in Angola's marine environmental protection framework, including the absence of systematic spill monitoring, inadequate emergency response capabilities, and limited public accountability for petroleum-related environmental damage. The technological solutions demonstrated here provide a foundation for addressing these governance deficiencies.

Future research directions emerging from this investigation include: (i) integration of machine learning classification algorithms to automate oil slick detection across large temporal datasets; (ii) coupling of SAR detection with oceanographic dispersion modeling for predictive spill trajectory

forecasting; (iii) correlation of spill events with operational records from Block 32 and other extraction zones to identify source attribution; (iv) long-term ecosystem monitoring to quantify recovery trajectories; and (v) expansion of the monitoring methodology to the entire Angolan coastline through inter-institutional collaboration with national universities and environmental agencies.

The present work confirms that remote sensing technology, when systematically applied through scientifically rigorous methodologies, provides an indispensable tool for environmental protection in petroleum-producing regions. As Angola continues to develop its hydrocarbon sector, the integration of SAR-based monitoring into operational environmental management represents both a technical imperative and a governance priority for sustainable coastal zone management.

REFERENCES

Afgatiani, P. M., Putri, F. A., Suhadha, A. G., & Ibrahim, A. (2020). Determination of Sentinel-2 spectral reflectance to detect oil spill on the sea surface. *Sustinere: Journal of Environment and Sustainability*, 4(3), 144-154. https://doi.org/10.22515/sustinere.jes.v4i3.115

Al-Ruzouq, R., Gibril, M. B. A., Shanableh, A., Kais, A., Hamed, O., Al-Mansoori, S., & Khalil, M. A. (2020). Sensors, features, and machine learning for oil spill detection and monitoring: A review. *Remote Sensing*, 12(20), 3338. https://doi.org/10.3390/rs12203338

Albuquerque, R. C. L. (2004). *Aplicacao do Sensoriamento Remoto e do Sistema de Informacoes Geograficas na deteccao de manchas de oleo na regiao do polo de exploracao de Guamare* (Master's thesis). Universidade Federal do Rio Grande do Norte.

Araujo, T. S. (2011). *Metodologia de utilizacao de dados de sensoriamento remoto em zonas costeiras sob influencia da industria petrolifera* (Master's thesis). Universidade Federal do Rio Grande do Norte.

Arslan, N. (2018). Assessment of oil spills using Sentinel 1 C-band SAR and Landsat 8 multispectral sensors. *Environmental Monitoring and Assessment*, 190(11), 663. https://doi.org/10.1007/s10661-018-7017-4

Baza, G. F. (2021). *A Interdependencia entre o Crescimento da Economia Angolana e as Receitas do Petroleo* (Master's thesis). Universidade da Beira Interior.

Boyd, D. S., & Danson, F. M. (2005). Satellite remote sensing of forest resources: Three decades of research development. *Progress in Physical Geography*, 29(1), 1-26.

Caruso, M. J., Migliaccio, M., & Tranfaglia, M. (2013). SAR oil spill observation and characterization: State of the art. *IEEE Geoscience and Remote Sensing Letters*, 10(1), 1-5.

Copernicus Programme. (2024). *Sentinel-1 User Handbook (Document SI-UCHB-ASD-054)*. European Space Agency.

Fingas, M., & Brown, C. E. (2018). Review of oil spill remote sensing. *Marine Pollution Bulletin*, 83(1), 9-19. https://doi.org/10.1016/j.marpolbul.2014.03.059

Henderson, F. M., & Lewis, A. J. (1998). Principles and applications of imaging radar. *Manual of Remote Sensing*, Volume 2 (3rd ed.). John Wiley & Sons.

Karathanassi, V., Topouzelis, K., & Pavlakis, P. (2006). Oil spill feature selection and classification using fully polarimetric SAR imagery. *International Journal of Remote Sensing*, 27(5), 903-914.

Lu, Y. (2003). Marine oil spill detection using SAR imagery: A case study in Southeast Asia. *Asian Journal of Geoinformatics*, 3(3), 25-34.

Migliaccio, M., Nunziata, F., & Buono, A. (2015). SAR polarimetry for oil spill observation and characterization: A review. *Remote Sensing of Environment*, 164, 209-213.

Pavlakis, P., Tarchi, D., & Sieber, A. J. (2001). On the monitoring of illicit vessel discharges using spaceborne SAR imagery: A reconnaissance study in the Mediterranean Sea. *Annals of Telecommunications*, 56(7-8), 700-718.

Roberts, J. (2011). Oil and gas. In *Remote Sensing of the Marine Environment* (pp. 233-258). CRC Press.

Salisbury, J. W., D'Aria, D. M., & Sabins, F. F. (1993). Thermal infrared remote sensing of crude oil slicks. *Remote Sensing of Environment*, 45(2), 225-231.

Tchissingui, A. (2015). *Aplicacao de SIG na caracterizacao do setor mineral da regiao de Jamba, Sul de Angola* (Master's thesis). Universidade Agostinho Neto.

Topouzelis, K. N. (2008). Oil spill detection by SAR images. *Progress in Oceanography*, 86(1-2), 109-119.

Torres, R., Snoeij, P., Geudtner, D., Bibby, D., Davidson, M., Attema, E., ... & Duesmann, B. (2012). GMES Sentinel-1 mission. *Remote Sensing of Environment*, 120, 9-24.